Electronic Supplementary Information

NMR Exchange Dynamics Studies of Metal-Capped Cyclodextrins Reveal Multiple Populations of Host-Guest Complexes in Solution

Elad Goren[a], Mark A. Iron[b], Yael Diskin-Posner[b], Alla Falkovich[b], Liat Avram[b], and Amnon Bar-Shir[a*]

[a] Department of Molecular Chemistry and Materials Science, Weizmann Institute of Science, Rehovot 7610001, Israel; [b] Department of Chemical Research Support, Weizmann Institute of Science, Rehovot 7610001, Israel

*Corresponding Author: amnon.barshir@weizmann.ac.il

SUPPLEMENTARY METHODS

Abbreviations

CD – Cyclodextrin, DTPA - diethylenetriaminepentaacetic acid, DTPAA - diethylenetriaminepentaacetic acid dianhydride, TEA – triethylamine, TFA – trifluoroacetic acid, DMSO – dimethyl sulfoxide, DDW - doubly distilled water.

Materials

$6^A,6^D$-diamino-$6^A,6^D$-dideoxy-β-cyclodextrin (**Diamino-β-CD**) was purchased from Arcos Organics. DTPAA and anhydrous DMSO were purchased from Sigma Aldrich. 4-trifluoromethylbenzylamine (**1**) and 3,5-difluorobenzylamine (**3**) were purchased from Alpha Aesar. 4-Fluorobenzylamine (**2**) and 2,6-difluorobenzylamine (**4**) were purchased from Apollo Scientific. Europium (III) chloride hexahydrate, anhydrous Dysprosium (III) chloride and Holmium (III) chloride hexahydrate were purchased from Strem Chemicals INC. Lanthanum (III) chloride heptahydrate was generously obtained from the lab of Prof. Boris Rybtchinski.

Synthetic Procedures

β-Cyclodextrin-DTPA (**β-CD-DTPA**)[1]

Under an inert N_2 atmosphere, a solution of **Diamino-β-CD** (100 mg, 82.92 μmol), DTPAA (29.63 mg, 82.92 μmol) and TEA (one drop) was stirred in anhydrous DMSO (2 mL) overnight. The solution was added dropwise to cold acetone (60 mL) while stirring, and the resulting white powder was collected after centrifugation (4˚C, 3000 rpm, 15 min). The crude solid was dissolved in a minimal volume of water and purified by reversed phase liquid chromatography. **β-CD-DTPA** was isolated as a white powder upon the removal of solvent (18.77 mg, 22.78% yield). ^{1}H-NMR (500.08, D_2O, Fig. S3e) δ 5.01-4.99 (multiple peaks, 7H), δ 4.23 (d, 2H), δ 4.14-3.18 (multiple peaks, 51H), δ 3.04-2.93 (m, 4H); ^{13}C-NMR (125.74 MHz, D_2O, Fig. S3f) δ 172.70, 170.33, 169.92, 166.54, 166.46, 102.51, 102.25, 102.17, 102.08, 101.84, 101.76, 101.52, 84.17, 84.14, 81.85, 81.77, 80.99, 80.88, 80.47, 73.33, 73.14, 73.10, 72.98, 72.89, 72.60, 72.41, 72.14, 72.09, 71.97, 71.94, 71.66, 71.58, 71.49, 70.97, 70.32, 60.49, 60.35, 60.08, 59.97, 59.82, 56.94, 56.36, 55.32, 55.29, 53.61, 53.36, 51.94, 50.38, 49.25, 40.81, 40.68; HRMS (Fig. S4): $C_{56}H_{91}O_{10}N_5$ calcd: m/z 1489.5200, found: 1490.5310 [M+H]$^+$, Δ 2.8 ppm, 1512.5140 [M+Na]$^+$, Δ 3.5 ppm.

[Lanthanide]-β-Cyclodextrin-DTPA (**Ln-β-CD**)

For each lanthanide, a solution of **β-CD-DTPA** (one equivalent) and $LnCl_3 \cdot XH_2O$ (one equivalent) in 15 mL DDW was refluxed for one hour while stirring. **Ln-β-CDs** (90-100% yield) were isolated as white powders upon the removal of solvent. HRMS: La-β-CD (Fig. S6): $C_{56}H_{88}O_{41}N_5La$ calcd: m/z 1626.22, found: 1626.4096 $[M+H]^+$, Δ 4.1 ppm, 1648.3916 $[M+Na]^+$, Δ 4.9 ppm. Dy-β-CD (Fig. S9): $C_{56}H_{88}O_{41}N_5Dy$ calcd: m/z 1650.42, found: 1673.4113 $[M+Na]^+$, Δ -1.9 ppm.

Methods

Reversed Phase High Performance Liquid Chromatography (RP-HPLC)

Analytical RP-HPLC analysis was performed using an Agilent Technologies 1260 Infinity quaternary pump LC system, equipped with a diode-array detector, through a C18 column. Preparative RP-HPLC was carried out using an Agilent 218 purification system, equipped with an auto-sampler, a C18 column, a UV-vis dual wavelength detector and a 440-LC fraction collector operated using OpenLab ChemStation software. Eluent A was 0.1% TFA in DDW and Eluent B was 90% acetonitrile and 0.1% TFA in DDW.

High-Resolution Electrospray Ionization Mass Spectrometry (ESI-Q-Tof-MS)

Analyses were carried out on a Waters Xevo G2-XS QTof Mass Spectrometer (Manchester, UK) with an electrospray ionization (ESI) source operating in the positive mode. Solutions were directly injected at a flow rate of 10 μL/min. All spectra were acquired in the mass range of 50 – 2000 m/z. Mass errors of the analyzed spectra are not larger than 5.0 ppm. The analyses were performed using a capillary voltage of 3.00 kV, a source temperature set at 120°C, and a cone voltage of 20V. The desolvation temperature was 280°C (for Eu-β-CD:1 and Dy-β-CD:1, Fig. S9) or 350°C and the desolvation gas (N_2) flow rate was 400 L/hr. All measurements were done using Leucine-Enkephalin (200 μg/μL, acetonitrile:H_2O containing 0.1% formic acid (1:1, v/v)) as a lockspray reference, at a flow rate of 10 uL/min. Data acquisition and recording were using Waters MassLynx version 4.2 software.

Computational Methods

Geometries were optimized using Grimme and coworkers' semiempirical method designed for geometries, frequencies and noncovalent interactions (GFN2-xTB)[2] using the code (xTB version 6.6.0) available from the authors. The solvent (water) environment was modelled using the analytical linearized Poisson–Boltzmann (ALPB) implicit solvation model.[3] The surface-excluded (Connolly) surfaces[4-7] were calculated using the Volarea plugin[8] to VMD version 1.9.4a51.[9]

UV-vis Spectroscopy

UV-Vis absorption spectra were recorded on an Agilent Cary 60 spectrophotometer using quartz cuvettes. DDW was used as a blank solution.

High-Resolution Nuclear Magnetic Resonance (NMR)

Sample Preparation: Unless stated otherwise, all NMR experiments were performed on solutions containing **Ln-β-CD** and **1** dissolved in D_2O (or in H_2O with a D_2O insert). Solutions were prepared in a 1:100 host-guest molar ratio with final concentrations of 150-170 μM and 15-17 mM respectively. All solutions were filtered using a MILLEX®-GV 0.22 μm PVDF filter unit prior to use.

Data Acquisition: All NMR experiments were performed on an 11.75 T AVANCEIII-HDNMR spectrometer (Bruker, Germany) with the sample temperature stabilized at 298K. The temperature was stabilized at 281, 288, 296 and 303 K for multipower experiments (Figs. S13-S14). *1D ^{1}H-NMR* spectra (500.08 MHz) were acquired for all samples prior to the ^{19}F-NMR experiments. *1D ^{19}F-NMR* spectra (470.54 MHz) were acquired for all host-guest samples, followed by longitudinal (T_1) and transverse (T_2) relaxation time evaluations.

Relaxation times: Prior to all ^{19}F-paraGEST experiments, in order to adjust the experimental parameters (saturation time and recovery time), both inversion recovery (IR, for evaluating T_1) and Car–Purcell–Meiboom–Gill (CPMG, for evaluating T_2) experiments were performed.

^{19}F-ParaGEST Experiments: Following a repetition time equals to three to five times the T_1 of the studied solution (as evaluated from IR experiments), a presaturation continuous wave (CW) radiofrequency (RF) pulse, with a duration of T_1, was applied prior to the 90° radiofrequency pulse. The saturation pulse strength (B_1) was set to 3.74 μT, unless stated otherwise. In order to acquire the full z-spectrum, the frequency of the presaturation pulse was swept from a positive offset ($+\Delta\omega$) to a negative offset ($-\Delta\omega$) relative to the resonance frequency of the free guest (the size of $\Delta\omega$ was defined based on the Ln used, as stated in each z-spectrum). In addition, a ^{19}F-NMR spectrum where the RF pre-saturation pulse was applied at a chemical shift of -0.21 ppm (off resonance to the frequency of the free guest), where a saturation transfer effect was not expected, was acquired as a reference spectrum.

Data Processing: The z-spectrum was plotted for each experiment by plotting the normalized intensity (S/S_0 or I/I_0) of the ^{19}F free guest signal at each frequency offset ($\Delta\omega$, relative to the frequency of the free guest), as a function of this applied presaturation pulse offset.

Diffusion Experiments: The ^{1}H diffusion NMR measurements were performed on an 11.75 T (500.08 MHz) AVANCE III HD NMR spectrometer (Bruker, Germany) equipped with a 50 Gauss/cm Z gradient system. A bipolar stimulated echo (STE) pulse sequence was used at 298 K. Diffusion experiments were performed with smoothed square (SMSQ.10.100) gradients, incremented from 2% to 98% in 16 linear steps with 64 scans were acquired for each gradient. The gradient duration was 4 ms, the diffusion time was 60 ms and the recycle delay was 3 s.
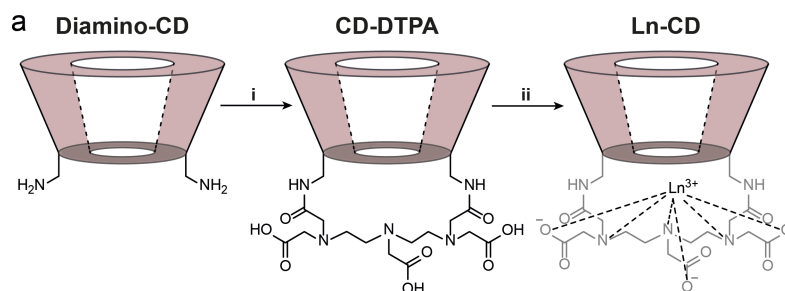
SUPPLEMENTARY FIGURES

Figure S1. Lanthanide-cyclodextrins (Ln-CDs) synthesis. The synthetic route used for the synthesis of Ln-CDs: (i) diethylenetriaminepentaacetic dianhydride (DTPAA) and trimethylamine (TEA) in anhydrous dimethyl sulfoxide (DMSO) at room temperature for 16 h; (ii) reflux with aqueous Lanthanide chloride (LnCl$_3$) for 1 h releasing hydrochloric acid (HCl);
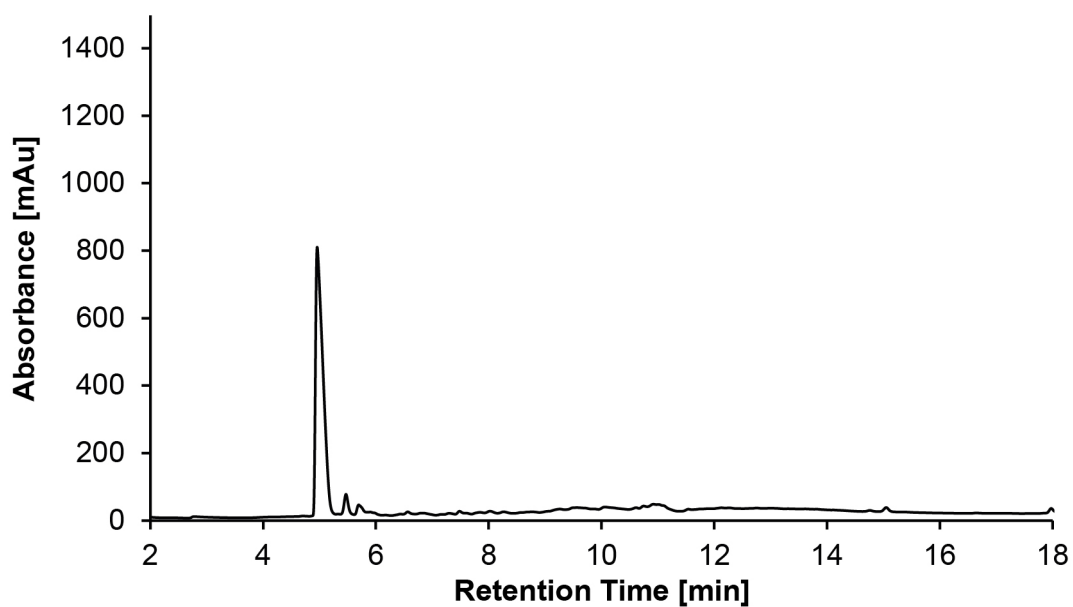

Figure S2. β-Cyclodextrin diethylenetriaminepentaacetic acid (β-CD-DTPA) absorbance at 220 nm. Measured by analytical High Performance Liquid Chromatography (HPLC).
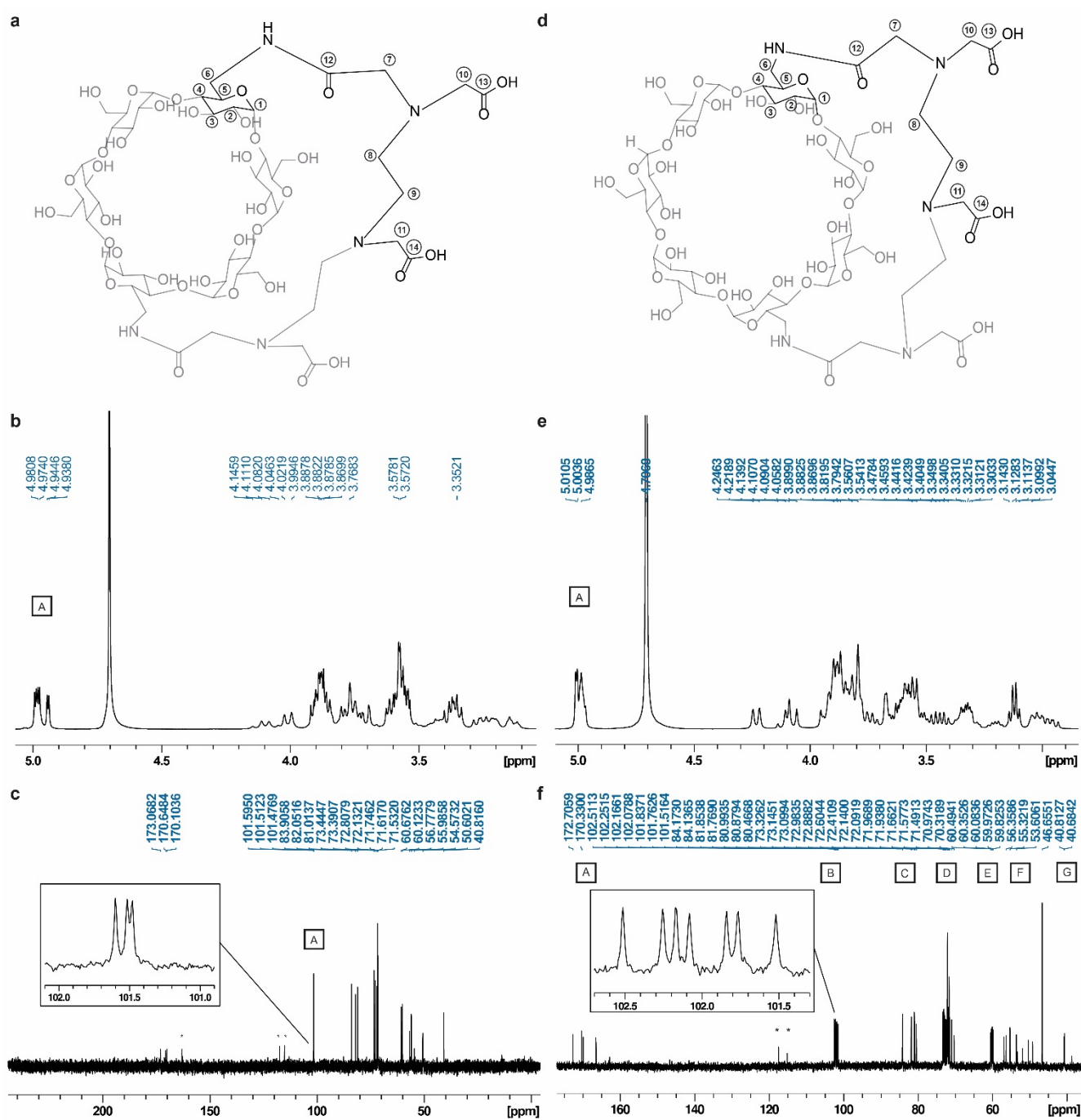
Figure S3. 1D-NMR spectra for α/β-CD-DTPA. (a) α-CD-DTPA structure and atom indications; (b) ^{1}H-NMR spectrum (500.08 MHz, D$_2$O) for α-CD-DTPA – A. peaks representing anomeric protons (H-1); (c) ^{13}C{^{1}H} NMR spectrum (125.74 MHz, D$_2$O) for α-CD-DTPA - A. peaks representing anomeric carbons (C-1); Inset – magnification of C-1 peaks. Panels a-c were adapted from previous work[10] ; (d) β-CD-DTPA structure and atom indications; (e) ^{1}H-NMR spectrum (500.08 MHz, D$_2$O) for β-CD-DTPA - A. peaks representing anomeric protons (H-1); (f) ^{13}C{^{1}H} NMR spectrum (125.74 MHz, D$_2$O) for β-CD-DTPA – A. Peaks representing carbonyls of the DTPA bridge (C-12-C-14), B. peaks representing C-1 in all units, C. peaks representing C-4 in all units, D. peaks representing C-2, C-3 and C-5 of all units, E. peaks representing C-6 of unsubstituted units, F. peaks representing carbons of the DTPA bridge (C-7-C-11 of the amine-substituted units, G. peaks representing C-6 of DTPA-substituted units; Inset – magnification of C-1 peaks; *Peaks representing contaminations.
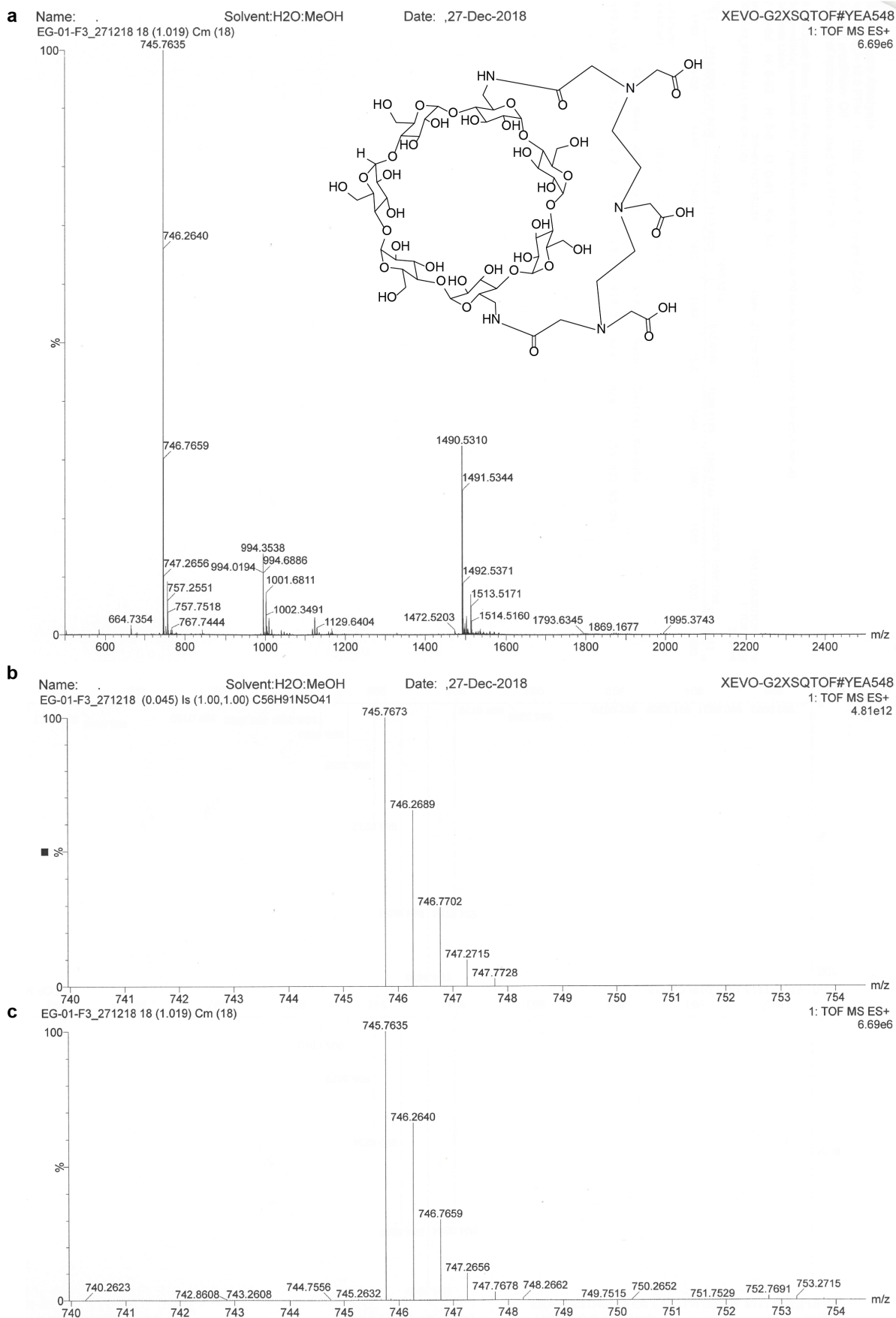
S5

Figure S4. MS spectrum and isotopic patterns for β-cyclodextrin diethylenetriaminepentaacetic acid (β-CD-DTPA). (a) Full spectrum; (b) simulated mass distribution for [M]²⁺; (c) experimental mass distribution for [M]²⁺.
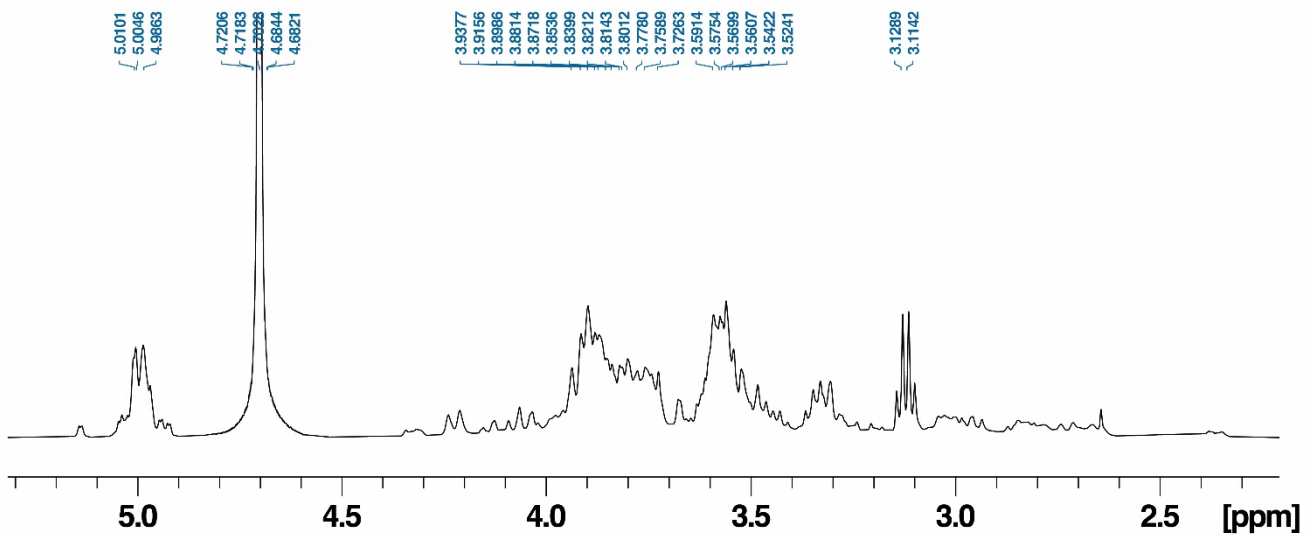
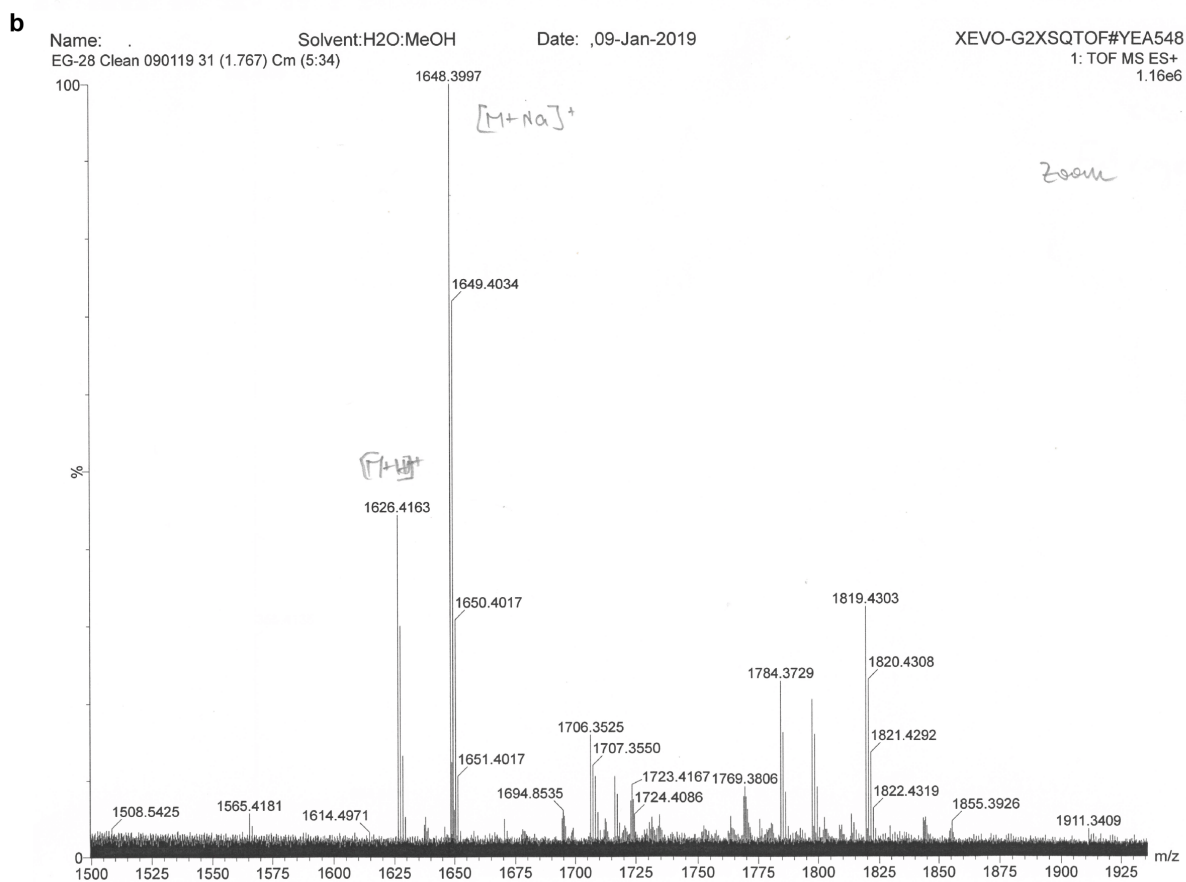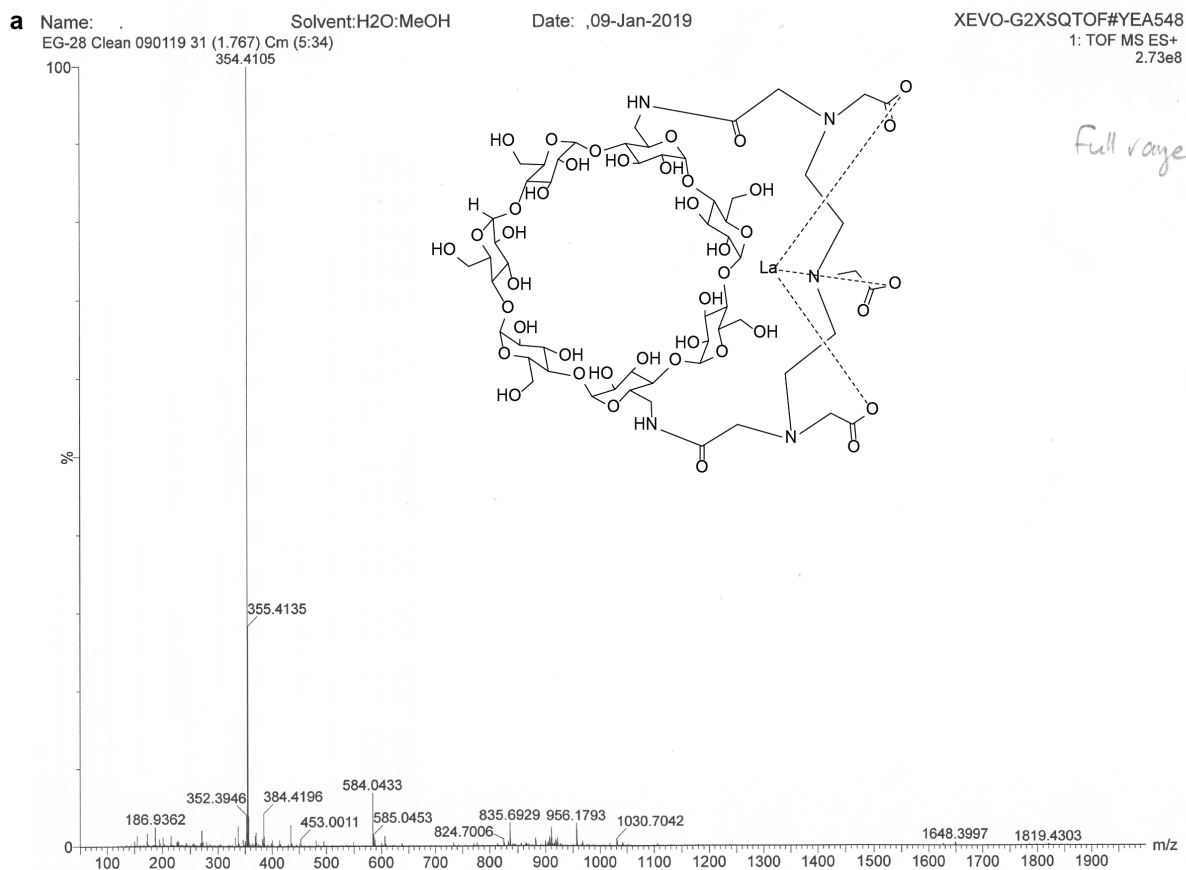**Figure S5.** ^{1}H-NMR spectrum (500.08 MHz, D_2O) for La-β-CD.

Figure S6. MS spectra for Lanthanum-β-cyclodextrin (La-β-CD). (a) Full spectrum; (b) magnification of the [M]⁺ peak range.

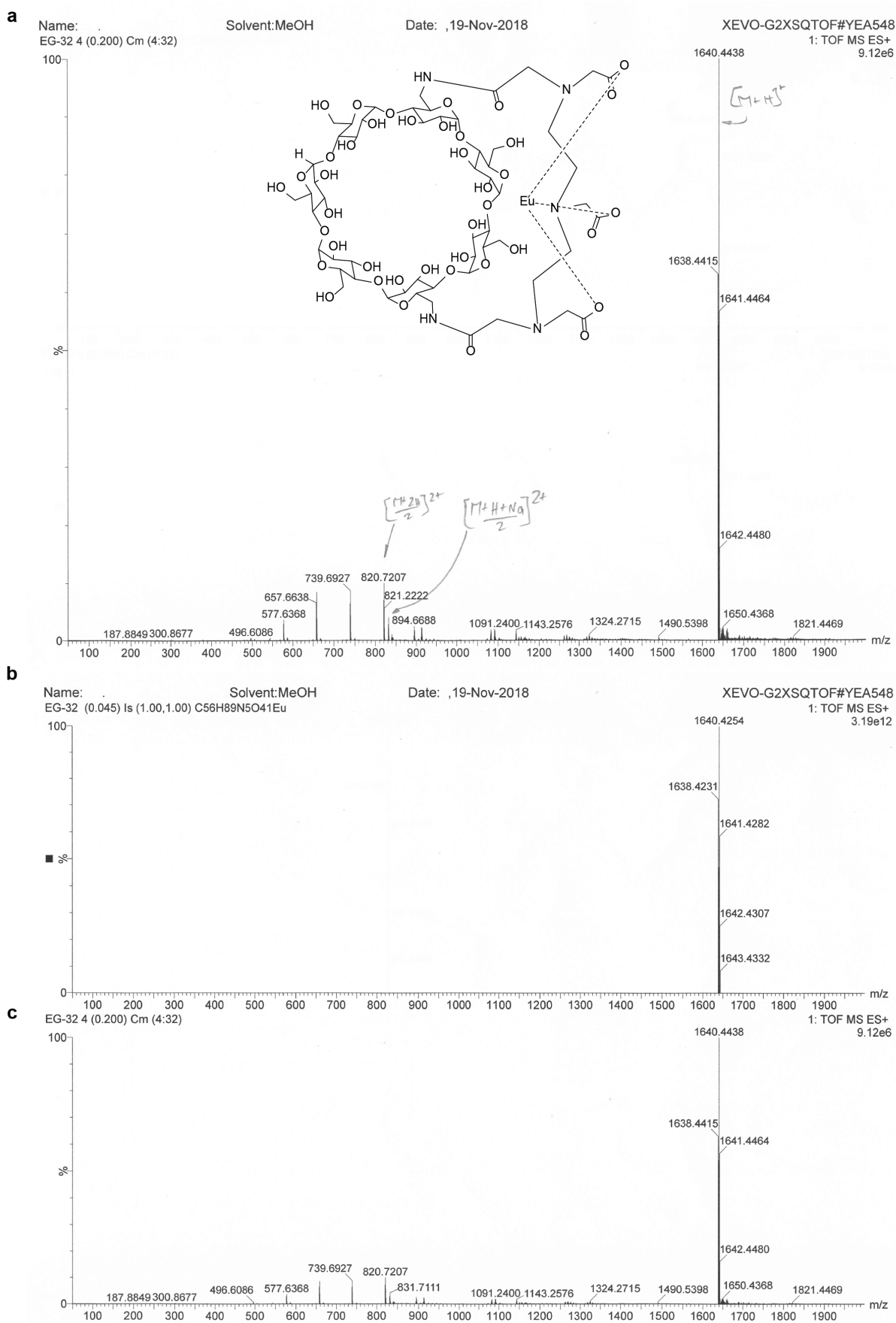**Figure S7. MS spectrum and isotopic patterns for Europium-β-cyclodextrin (Eu-β-CD).** (a) Full range spectrum; (b) simulated mass distribution for [M]+; (c) experimental mass distribution for [M]+.
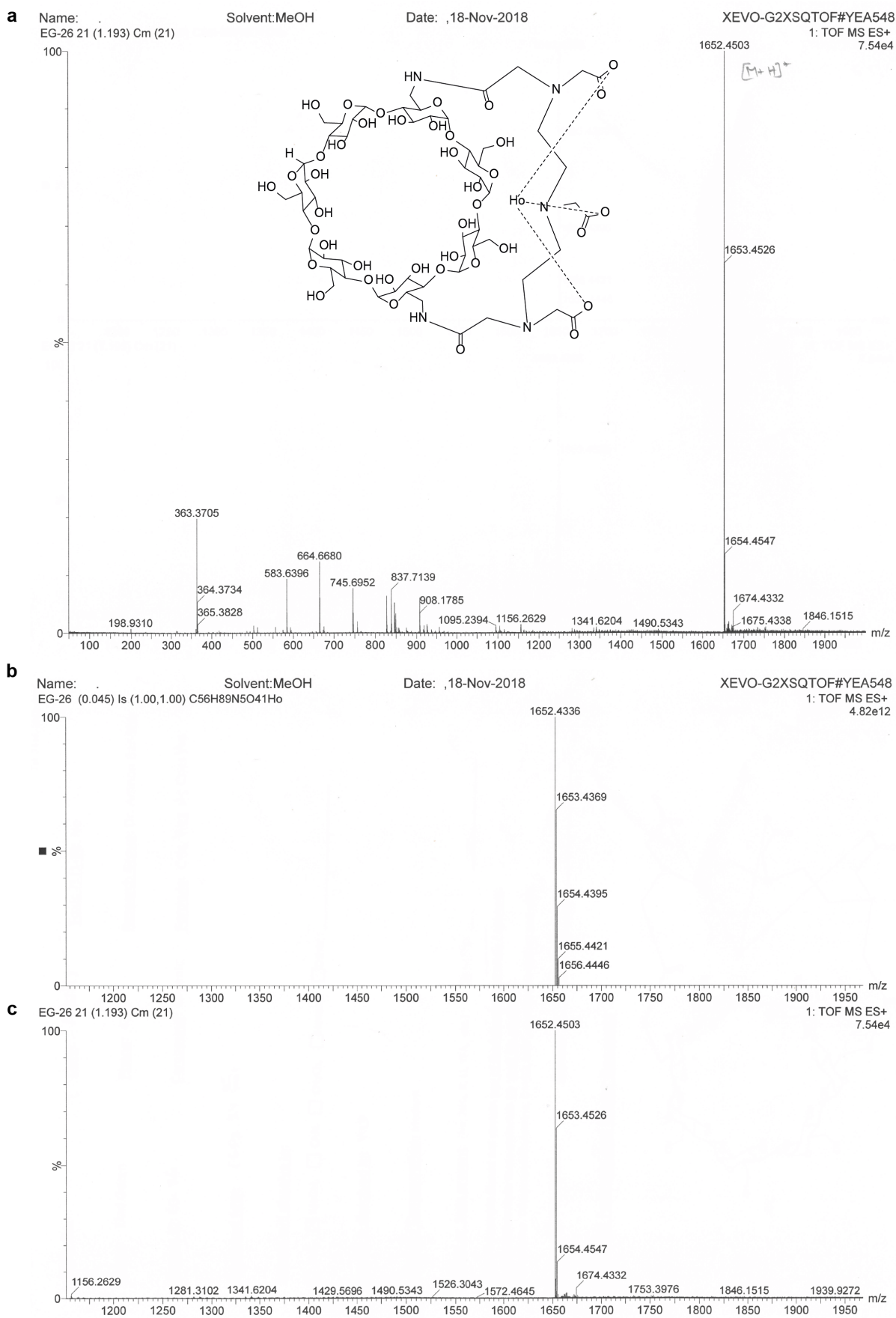
Figure S8. MS spectrum and isotopic patterns for Holmium-β-cyclodextrin (Ho-β-CD). (a) Full spectrum; (b) simulated mass distribution for [M]+; (c) experimental mass distribution for [M]+.
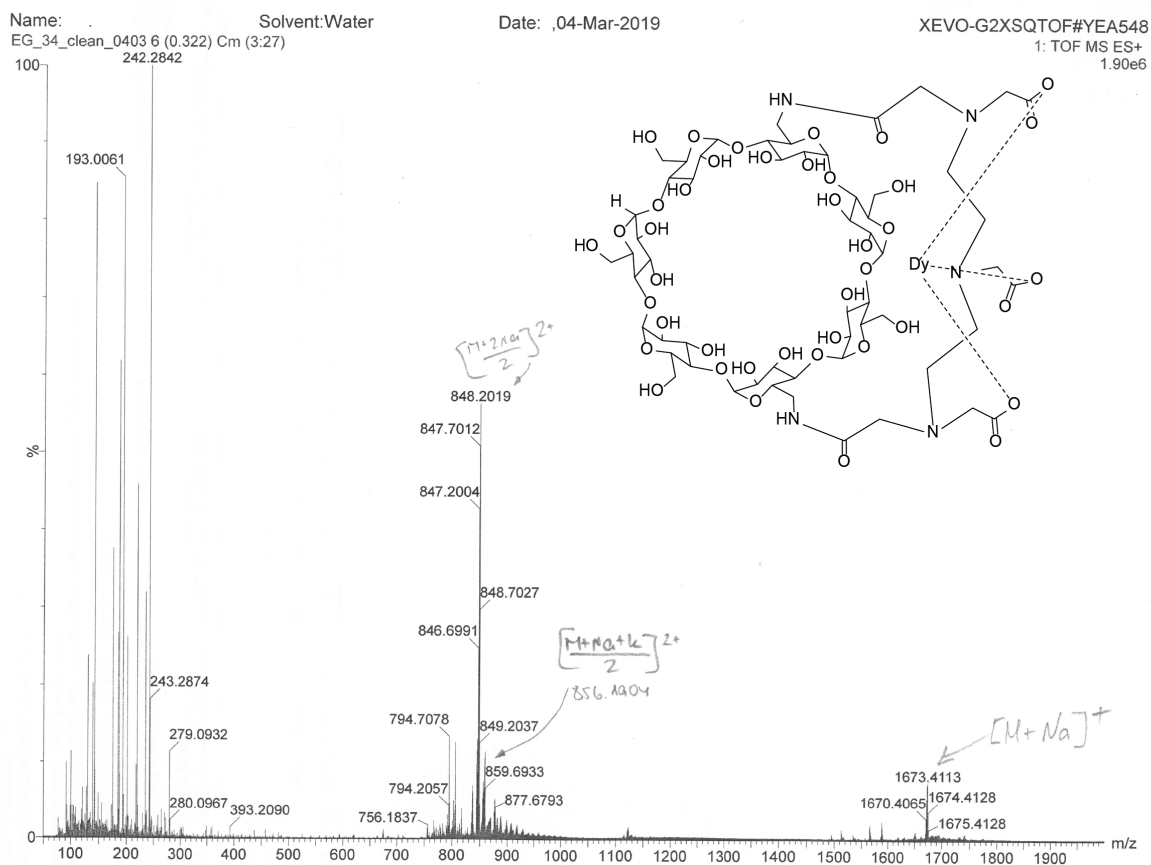
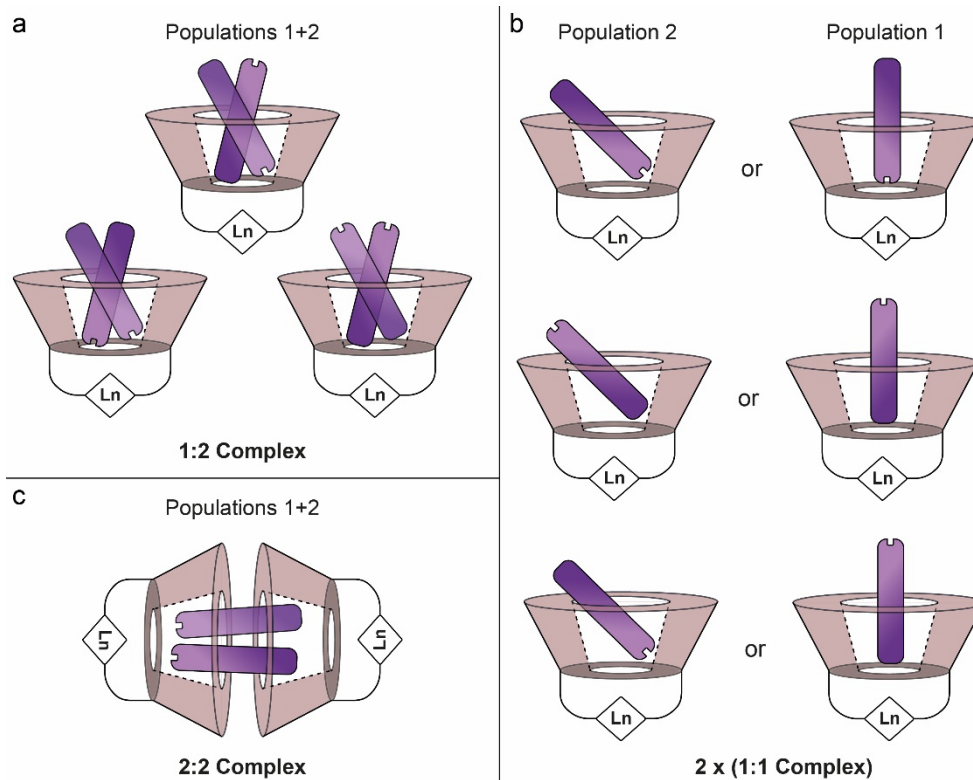**Figure S9. MS spectrum for Dysprosium-β-cyclodextrin (Dy-β-CD).**

Figure S10. Schematic illustrations of additional possible carceroisomers of Ln-β-CD:1 inclusion complexes. Carceroisomers for (**a**) 1:2, (**b**) 1:1 and (**d**) 2:2 host-guest stoichiometries.
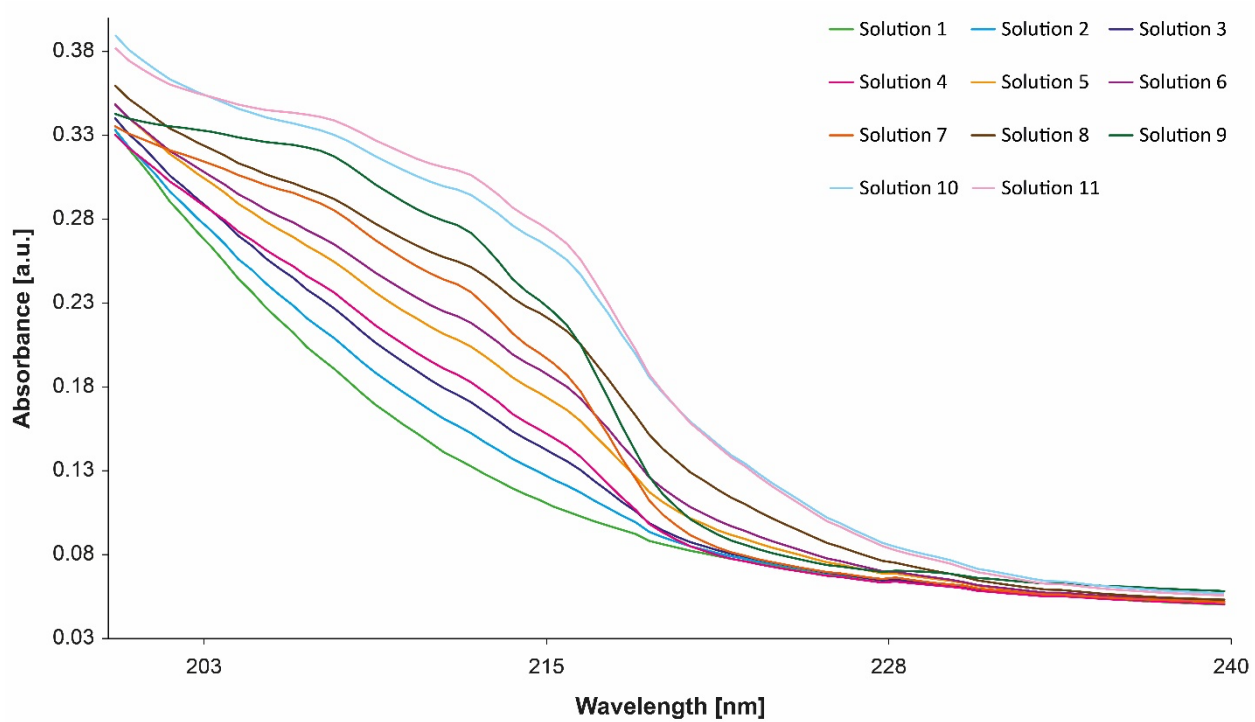
Figure S11. UV-vis absorbance spectrum used for Jobs plot calculation (Figure 5g). Details are given in Table S2.
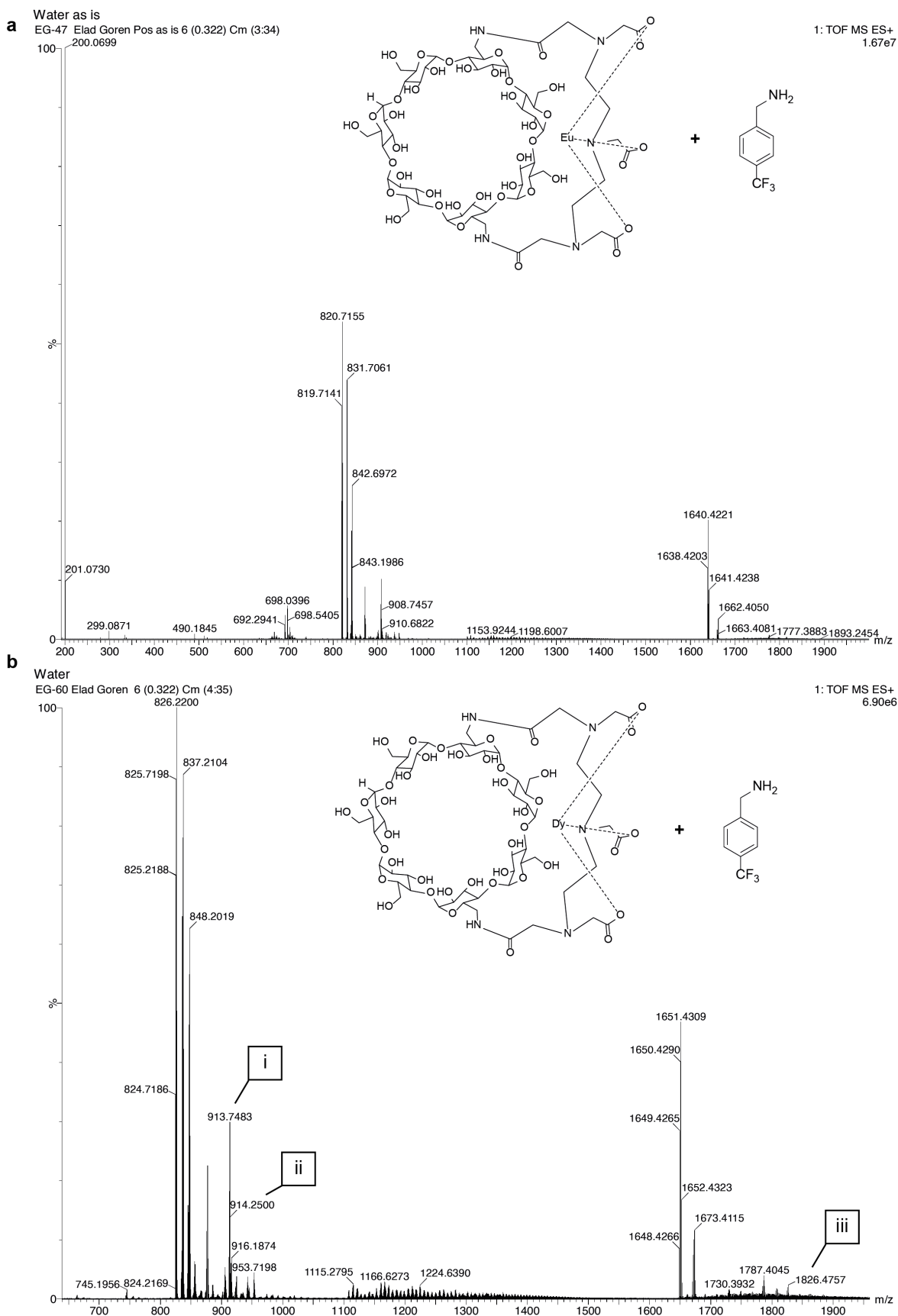
Figure S12. MS spectra for Lanthanide-β-cyclodextrin (Ln-β-CD):1. (a) Eu-β-CD:**1**; (b) Dy-β-CD:**1**. i = Mass of [1:1 complex + 2H]$^{2+}$, ii = Mass of [1:1 complex + 3H]$^{2+}$, iii = Mass of [1:1 complex + H]$^{+}$.

Figure S13. ^{19}F-paraGEST multipower fittings for Dysprosium-β-cyclodextrin (Dy-β-CD):1 at different temperatures.
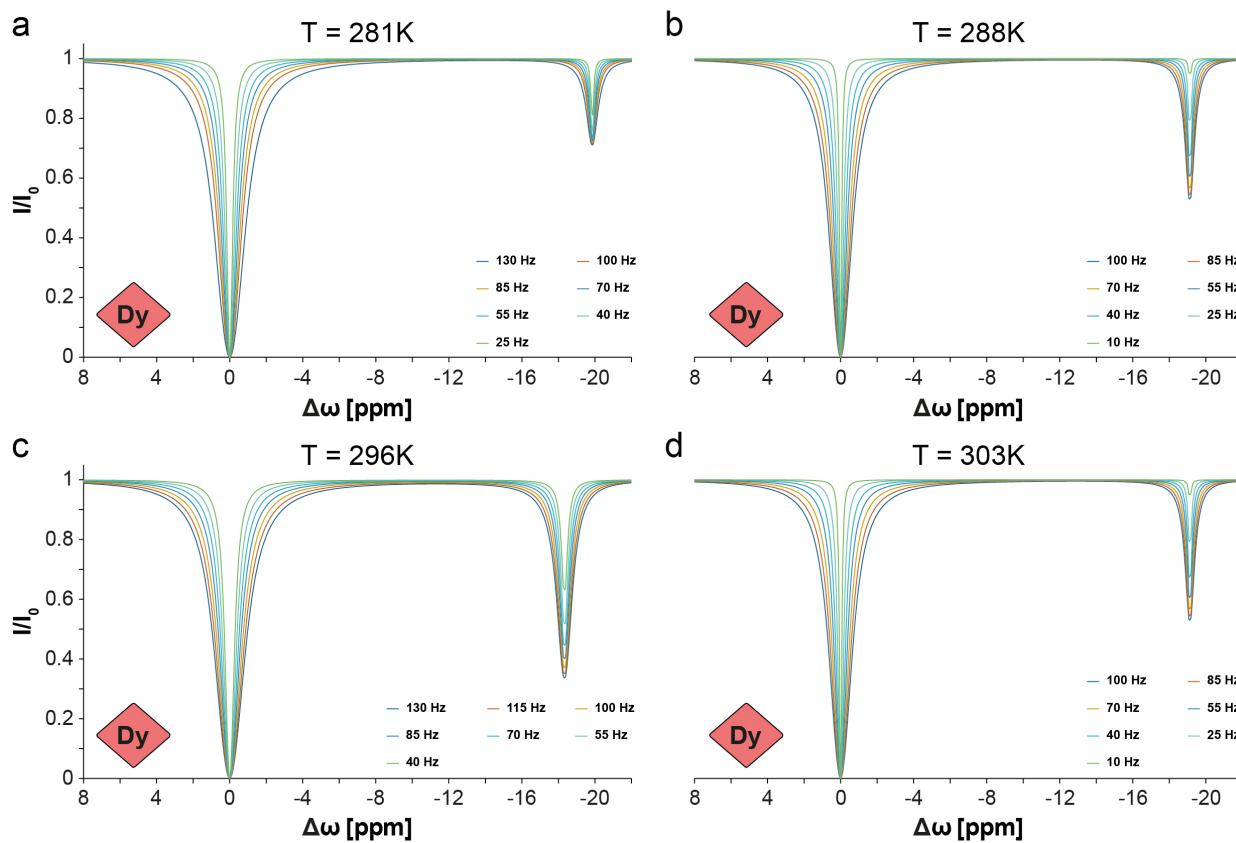
Figure S14. ^{19}F-paraGEST multipower fittings for Dysprosium-α-cyclodextrin (Dy-α-CD):1 at different temperatures.

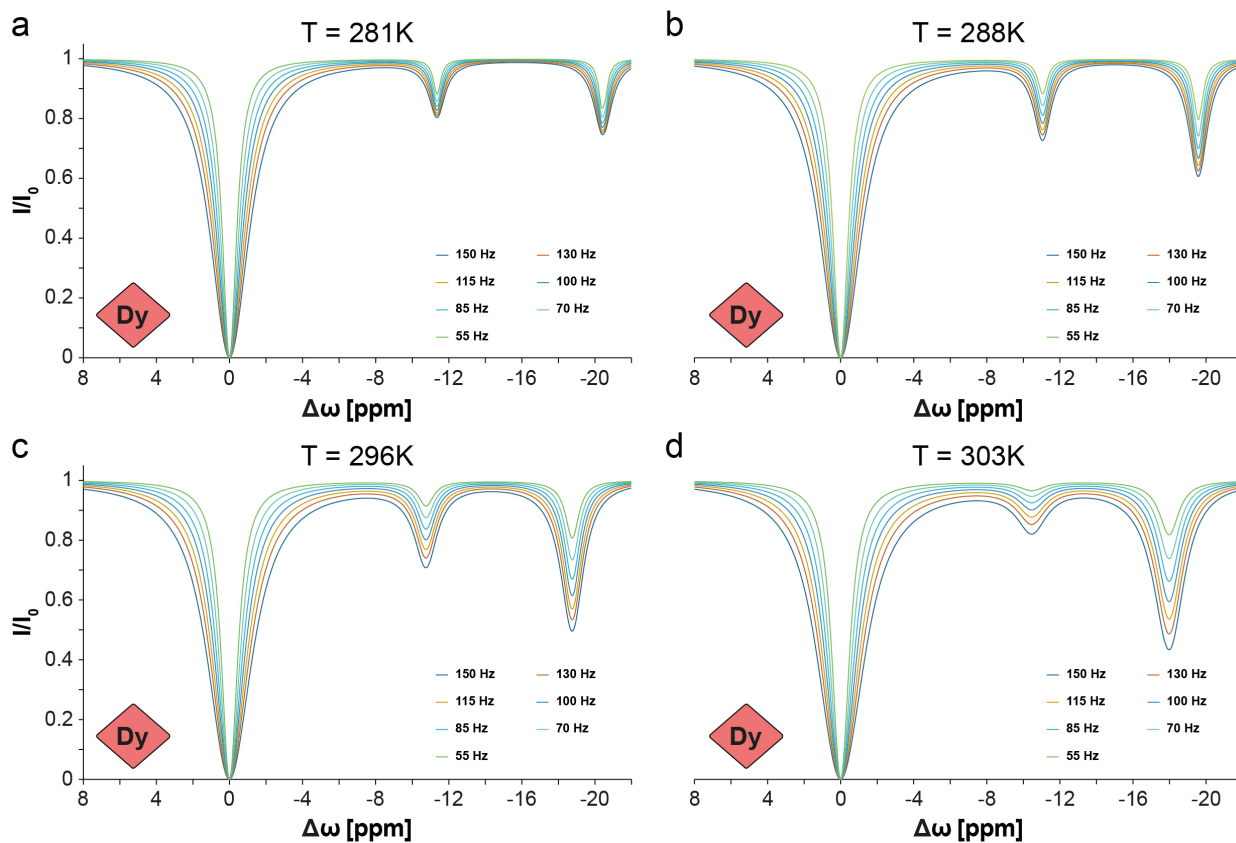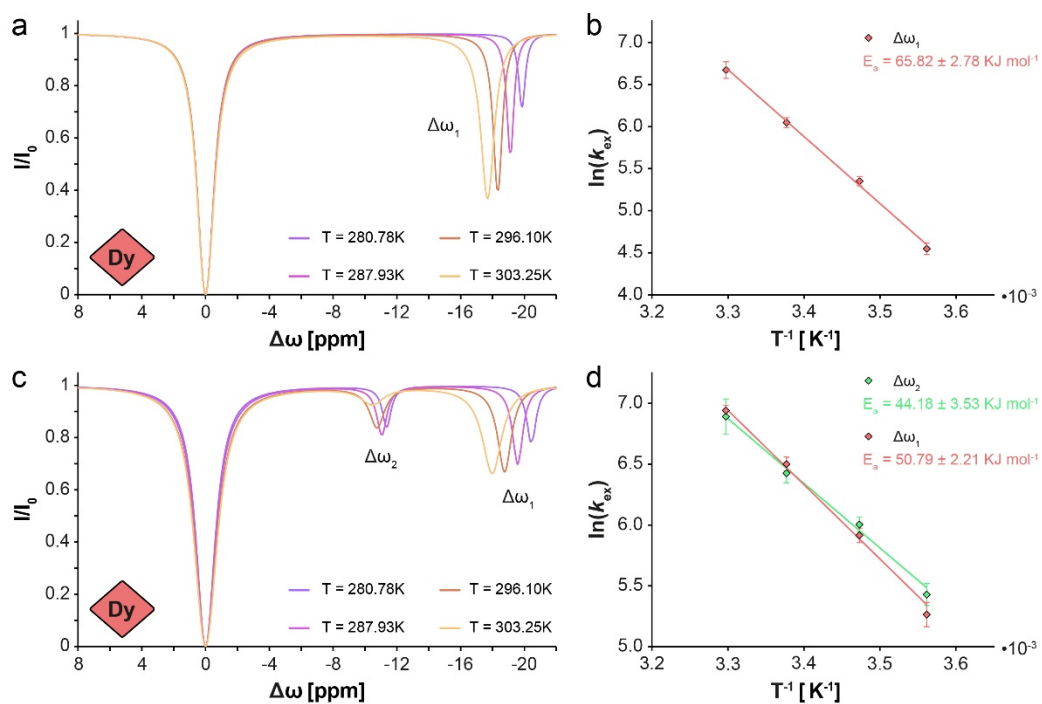**Figure S15. ^{19}F-ParaGEST multipower fittings at different temperatures and effect-specific activation energy calculation.** (a) z-spectra fittings for Dy-α-CD:1 at a saturation power of 85 Hz at different temperatures; (b) Arrhenius plot used to estimate the activation energy for a single ^{19}F-paraGEST effect; (c) z-spectra fittings overlay for Dy-β-CD:1 at a saturation power of 85 Hz at different temperatures; (d) Arrhenius plots used to estimate the activation energy calculation for the two ^{19}F-paraGEST effects.

SUPPLEMENTARY TABLES

Table S1. The chemical shift offsets ($\Delta\omega$, relative to the free guest) of the ^{19}F-paraGEST effects for guests **2**-**4**.

Guest	2		3		4	
	$\Delta\omega_1$ [ppm]	$\Delta\omega_2$ [ppm]	$\Delta\omega_1$ [ppm]	$\Delta\omega_2$ [ppm]	$\Delta\omega_1$ [ppm]	$\Delta\omega_2$ [ppm]
Dy-α-CD:Guest	-20.6	-	-28.5	-	-61.9	-
Dy-β-CD:Guest	-21.4	-13.5	-26.2		-55.6	-49.2

Table S2. Content of measured solutions and their absorbance (213nm) used for Jobs Plot. Host = Lanthanum-β-cyclodextrin (La-β-CD) and Guest = **1**.

	Guest Solution [mL]	Host Solution [mL]	Final Guest Concentration [μM]	Final Host Concentration [μM]	[Guest] / ([Guest]+[Host])	Guest Absorbance	ΔA	ΔA·[Guest] / ([Guest]+[Host])
Solution 1	0	3	0	100	0	0.132625952	0.173635229	0
Solution 2	0.3	2.7	10	90	0.1	0.152345792	0.15391539	0.015391539
Solution 3	0.6	2.4	20	80	0.2	0.17083694	0.135424241	0.027084848
Solution 4	0.9	2.1	30	70	0.3	0.182686195	0.123574987	0.037072496
Solution 5	1.2	1.8	40	60	0.4	0.203884587	0.102376595	0.040950638
Solution 6	1.5	1.5	50	50	0.5	0.218088806	0.088172376	0.044086188
Solution 7	1.8	1.2	60	40	0.6	0.236389786	0.069871396	0.041922837
Solution 8	2.1	0.9	70	30	0.7	0.251344144	0.054917038	0.038441926
Solution 9	2.4	0.6	80	20	0.8	0.271761984	0.034499198	0.027599359
Solution 10	2.7	0.3	90	10	0.9	0.294374853	0.011886328	0.010697696
Solution 11	3	0	100	0	1	0.306261182	0	0

Table S3. Measured diffusion coefficients of different ^1H-NMR peaks of **1**, La-β-CD and water in samples containing only **1**, only La-β-CD, and both in a 5:1 ratio.

Compound	Chemical Shift [ppm]	D [·10^{-5} cm^2/sec]		
		Host Only	Guest Only	Host:Guest
Guest 1	7.714	-	0.543	0.514
	7.536	-	0.543	0.531
H$_2$O	4.700	1.590	1.593	1.622
La-β-CD	3.886	0.2016	-	0.204
	3.573	0.2031	-	0.204

Table S4. Normalized measured diffusion coefficients of different ^{1}H-NMR peaks of **1**, La-β-CD in samples containing only **1**, only La-β-CD, and both in a 5:1 ratio (averaged from the values presented in Table S3).

	Normalized D [$\cdot 10^{-5}$ cm^2/sec]		
	Host only	**Guest only**	**Host:Guest**
Guest 1	-	0.682 ± 0.001	0.644 ± 0.010
La-β-CD	0.255 ± 0.001	-	0.252 ± 0.001

SUPPLEMENTARY REFERENCES

1. M. A. Mortellaro and D. G. Nocera, *J. Am. Chem. Soc.*, 1996, **118**, 7414-7415.
2. C. Bannwarth, S. Ehlert and S. Grimme, *J. Chem. Theory Comput.*, 2019, **15**, 1652-1671.
3. S. Ehlert, M. Stahn, S. Spicher and S. Grimme, *J. Chem. Theory Comput.*, 2021, **17**, 4250-4261.
4. F. M. Richards, *Annu. Rev. Biophys. Bioeng.*, 1977, **6**, 151-176.
5. M. L. Connolly, *J. Appl. Crystallogr.*, 1983, **16**, 548-558.
6. T. J. Richmond, *J. Mol. Biol.*, 1984, **178**, 63-89.
7. M. L. Connolly, *J. Mol. Graphics*, 1993, **11**, 139-141.
8. J. V. Ribeiro, J. A. C. Tamames, N. N. F. S. A. Cerqueira, P. A. Fernandes and M. J. Ramos, *Chem. Biol. Drug Des.*, 2013, **82**, 743-755.
9. W. Humphrey, A. Dalke and K. Schulten, *J. Mol. Graphics*, 1996, **14**, 33-38.
10. E. Goren, L. Avram and A. Bar-Shir, *Nat. Commun.*, 2021, **12**, 3072.